INTERPLAY BETWEEN PARTICLE AND CORE EXCITATIONS IN ^{133}Sb*

G. Bocchi[a,b], S. Leoni[a,b] B. Fornal[c], G. Colò[a,b]
P.F. Bortignon[a,b], D. Bazzacco[d], A. Blanc[e], S. Bottoni[a,b]
N. Cieplicka-Oryńczak[b,c], F.C.L. Crespi[a,b], G. De France[f]
M. Jentschel[e], U. Koster[e], C. Michelagnoli[e,f], P. Mutti[e]
J.-M. Régis[g], G. Simpson[h], T. Soldner[e], B. Szpak[c], C.A. Ur[d,i]
W. Urban[j]

[a]Dipartimento di Fisica, Università degli Studi di Milano, Milano, Italy
[b]INFN sezione di Milano, via Celoria 16, 20133, Milano, Italy
[c]The H. Niewodniczański Institute of Nuclear Physics PAN
Radzikowskiego 152, 31-342 Kraków, Poland
[d]INFN Sezione di Padova, Padova, Italy
[e]ILL, 71 Avenue des Martyrs, 38042 Grenoble CEDEX 9, France
[f]GANIL, BP 55027, 14076 Caen CEDEX 5, France
[g]IKP, Univ. of Cologne, Zulpicher Str. 77, 50937 Köln, Germany
[h]LPSC, 53 Avenue des Martyrs, 38026 Grenoble, France
[i]ELI–NP Măgurele-Bucharest, Romania
[j]Faculty of Physics, Univ. of Warsaw, Hoża 69, 00-681 Warszawa, Poland

(Received December 14, 2016)

The γ decay of the one-proton valence nucleus ^{133}Sb is studied using the cold-neutron induced fission of ^{235}U and ^{241}Pu targets. The experiment is performed at the ILL reactor in Grenoble, using a highly efficient HPGe array, also coupled to fast $LaBr_3$(Ce) scintillators. High-spin excited states above the 16.6 μs isomer are observed, and the lifetime of the $13/2^+$ and $15/2^+$ states is measured by fast-timing techniques, revealing a complex nature of the wave functions. The experimental results are well-interpreted by a newly developed microscopic model which takes into account the coupling between the valence proton and excitations (both collective and non-collective) of the doubly magic ^{132}Sn core.

DOI:10.5506/APhysPolB.48.595

* Presented at the Zakopane Conference on Nuclear Physics "Extremes of the Nuclear Landscape", Zakopane, Poland, August 28–September 4, 2016.

1. Introduction

In nuclei with one- or two-valence particles outside a magic core, the lowest structures are dominated by the couplings with excitations of the core, of both collective (phonons) and less collective nature. The understanding of these couplings is of primary importance, being responsible, to a large extent, for a series of basic phenomena, such as the anharmonicities of vibrational spectra, the quenching of spectroscopic factors and the damping of giant resonances [1]. So far, studies of particle-core excitations considered mainly couplings with collective phonons and relied, to a large extent, on phenomenological models [1–4].

In this work, we concentrate on the benchmark region around ^{132}Sn, which is one of the best doubly magic cores and exhibits low-lying collective and non-collective excitations. In particular, we investigate the nature of particle–core excitations in the corresponding one-valence-proton nucleus ^{133}Sb, populated via cold-neutron induced fission reactions. First, we aimed at identifying, experimentally, new high-spin yrast states above the long-lived 16.6 μs isomer. Then, we studied transition probabilities through lifetime measurements of selected states. In order to interpret the data, a new microscopic and self consistent model was developed, containing particle couplings to core excitations of various nature.

2. Experimental setup and data analysis

The EXILL campaign took place in 2012–2013 at the PF1B [5] cold-neutron facility at the Institute Laue–Langevine (Grenoble, France). The ILL reactor is the world's brightest continuous neutron source with an in-pile flux up to 1.5×10^{15} neutrons s^{-1} cm^{-2}, providing of the order of 10^8 neutrons s^{-1} cm^{-2} on target, after collimation. The main part of the campaign consisted of two long runs of neutron induced fission of ^{235}U and ^{241}Pu targets, giving access to several nuclei with limited spectroscopic information.

In this contribution, we focus on the analysis of the one-valence proton nucleus ^{133}Sb, which was investigated by making use of two different detector setups [6]. The first one consisted of 8 EXOGAM clovers (at 90° with respect to the beam direction), 6 large coaxial detectors from GASP (at 45°) and 2 ILL-Clover detectors (at 45° and 180° with respect to the beam direction and the GASP detectors, respectively) with a total photopeak efficiency of about 6%. In the second configuration, the GASP and ILL detectors were replaced by 16 LaBr$_3$(Ce) crystals, from the FATIMA Collaboration, for lifetime measurements by fast-timing techniques. A digital data acquisition, triggerless, allowed event rates up to 0.84 MHz to be handled.

The first part of the analysis was devoted to the search for new high-spin yrast states, focusing on the region above the long-lived 16.3 μs, $21/2^+$ isomer [7], so far unexplored. The $21/2^+$ isomer decays via a cascade of five transitions: an unknown isomeric transition with $E_\gamma < 30$ keV followed by 62, 162, 1510 and 2792 keV γ rays that feed the $7/2^+$ ground state. Therefore, the search for high-spin structures of ^{133}Sb started by considering coincidences between two classes of γ rays: *(i)* prompt γ rays — coincident (within 200 ns) with a fission event (defined by γ-ray multiplicity equal or larger than 4, within 200 ns) and *(ii)* delayed γ rays emitted within 20 μs after the fission event and coincident (within 200 ns) with at least one of the four known transitions de-exciting the $21/2^+$ isomer. This allowed us to investigate prompt–delayed and prompt–prompt coincidences. Examples of delayed (panel (a)) and prompt (panel (b)) spectra, obtained with the ^{241}Pu target, are shown in Fig. 1. A crucial point in the analysis was the comparison of the results obtained with the two different targets, ^{235}U and

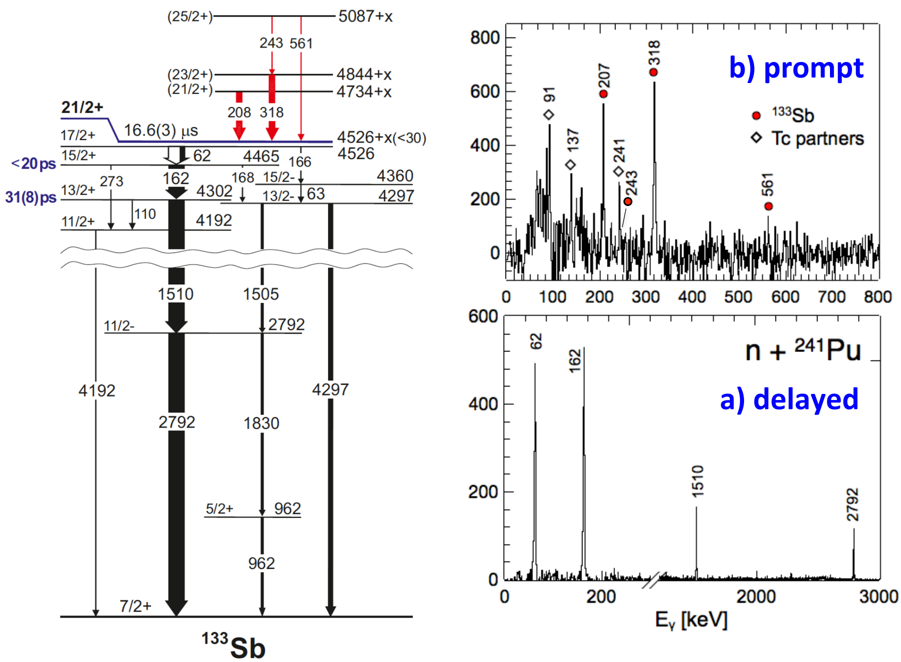

Fig. 1. (Color on-line) Left: Experimental level scheme of ^{133}Sb. In black, the decay below the long lived $21/2^+$ isomer. In grey/red, newly identified transitions, above the isomer. Right: (a) γ spectrum obtained requesting coincidences (within 200 ns) among the 162, 1510 and 2792 keV transitions depopulating the $21/2^+$ isomer; (b) spectrum of γ events in prompt coincidence with fission and with delayed transition of ^{133}Sb, depopulating the $21/2^+$ isomer. Both panels refer to ^{241}Pu data.

^{241}Pu. In both data sets, γ rays at 207.9(4), 318(4) and 561(1) keV were clearly observed as preceding the $21/2^+$ isomer, and a weak line at 243 keV was also found to appear in coincidence with the 318 keV transition. The extend level scheme, up to spin $25/2^+$, is given in the left part of Fig. 1.

In the second part of the work, the lifetime of the $13/2^+$ and $15/2^+$ states was measured with the LaBr$_3$(Ce) scintillators, using the fast timing technique [8]. The analysis was based on triple coincidence events, within a time windows of 200 ns, in which two γ rays are detected in the scintillators and the third one in the HPGe array. In the present case, by setting a very selective gate on the 2792 keV line of ^{133}Sb recorded in the HPGe, a (E_{γ_1}, E_{γ_2}, Δt) histogram was constructed, being Δt the time difference between γ rays with E_{γ_1} and E_{γ_2} energies measured in the LaBr$_3$(Ce) detectors. The analysis of the time spectra obtained from the delayed and anti-delayed coincidence are shown in Fig. 2. All spectra are background subtracted by considering a two-dimensional gate in the energy plane, in the region of the coincidence peak (as shown in the insets). The time difference ΔC between the centroids of the time distributions, after correction for the Prompt Response Difference, provides the values of $T_{1/2} = 31(8)$ ps and < 20 ps for the $13/2^+$ and $15/2^+$, respectively. Taking into account the decay branches from the two levels [7], B(M1) reduced transition probabilities were extracted for the $15/2^+ \rightarrow 13/2^+$ and $13/2^+ \rightarrow 11/2^+$ transitions. A large difference between the two values was obtained (> 0.24 and 0.0042(15) W.u.), clearly pointing to a complex structure for these levels.

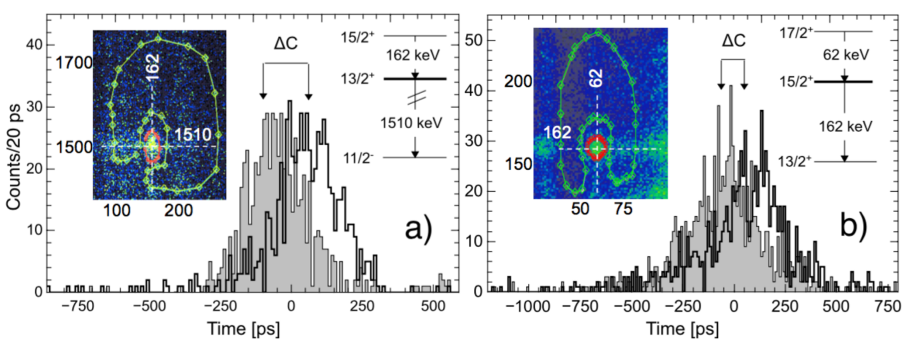

Fig. 2. Time spectra employed in the lifetime analysis of the $13/2^+$ (left) and $15/2^+$ (right) states. Dark (light) histograms are the delayed (anti-delayed) time difference for the cascades shown in the right part of each picture. Examples of two-dimensional background selections are given in the insets.

In order to interpret the experimental results, a new microscopic approach, named Hybrid Configuration Mixing Model (HCM), was developed [9]. The aim of the model is to describe states with different degrees of collectivity by solving the Hamiltonian $H = H_0 + V$ with

$$H_0 = \sum_j \epsilon_j a_j^\dagger a_j + \sum_{NJM} \hbar\omega_{NJ} \Gamma_{NJM}^\dagger \Gamma_{NJM}\,, \tag{1}$$

$$V = \sum_{jmj'm'} \sum_{NJM} \frac{\langle jm||V||j'm', NJM\rangle}{\sqrt{2j+1}} a_{jm} \left[a_{j'm'}^\dagger \otimes \Gamma_{NJ}^\dagger\right]_{jm}\,, \tag{2}$$

where we used jm instead of $nljm$ for the usual quantum number of the single-particle states, and each spin/parity $J^\pi M$ of the core excitations have been labelled with an index N and simply written in the form NJM. a and $a^\dagger$ are the usual fermion annihilation and creation operators, while the notation Γ and $\Gamma^\dagger$ is used for boson operators. ϵ and $\hbar\omega$ are the energies of single-particles and RPA solutions respectively.

The calculation has no free parameters and is self-consistent: single-particle, phonons and coupling matrix elements are calculated using the same Skyrme SkX interaction [10]. The model is found to reproduce well the energy sequence of the high-spin states observed experimentally. In addition, it provides an explanation for the large experimental difference in B(M1) values, in terms of wave function composition. The latter evolves from complex to non-collective character, with increasing spin, as shown in the right-hand side of Fig. 3. In particular, while the low-spin states are

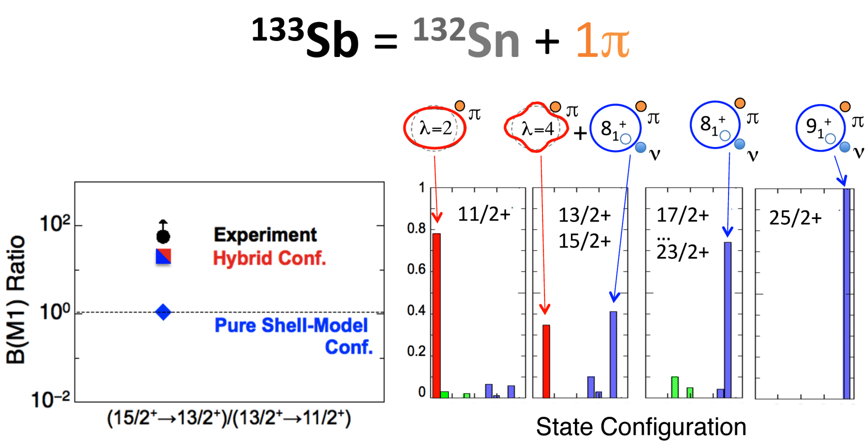

Fig. 3. Left: A comparison of the experimental ratio between B(M1) values and theory predictions from the "hybrid" model and pure shell model calculations. Right: Predictions of the "hybrid" model for the components of each lowest state with amplitude larger than 0.01 (a schematic representation is given on top).

dominated by the $g_{7/2}$ proton coupled to the 2^+ core excitation, the highest spin excitations arise mostly from the valence proton coupled to the neutron $h^{-1}_{11/2}f_{7/2}$ non-collective core excitation. Intermediate states show instead a fragmented wave function, involving several core excitations, both collective (4^+) and non-collective (8^+). As a result, the model provides the values of 0.021 W.u. and 0.001 W.u. for the B(M1) transition probabilities relative to the $15/2^+ \to 13/2^+$ and $13/2^+ \to 11/2^+$ transitions, respectively. Despite the discrepancy with the experimental results, the large B(M1)'s ratio (≈ 20) is in a qualitative agreement with the experimental one (larger than 60), as shown in the right-hand side of Fig. 3, at variance from a simple shell-model picture [7].

3. Conclusion

In summary, new high-spin yrast states in the one-valence proton nucleus ^{133}Sb were observed above the $21/2^+$, 16.6 μs isomer, up to $(25/2^+)$. Lifetimes of the $13/2^+$ and $15/2^+$ excited states were also measured. The structure of ^{133}Sb was described by a new "hybrid" microscopic model, including couplings with various types of core excitations. The model is found to reproduce very well the energies of the excited states and provides an explanation for the large difference in M1 strength for transitions connecting neighbouring medium-spin yrast states, as a result of a mixed composition of the wave functions of the states. The present work gives new perspectives in the study of complex excitations around doubly magic systems.

The authors thank the technical services of the Institute Laue–Langevin, LPSC, and GANIL for supporting the EXILL campaign. The EXOGAM Collaboration and the INFN-Legnaro are acknowledged for the loan of Ge detectors. This work is supported by the Polish National Science Centre under contracts No. 2014/14/M/ST2/00738, and No. 2013/08/M/ST2/00257.

REFERENCES

[1] A. Bohr, B.R. Mottelson, *Nuclear Structure*, Vols. I and II, W.A. Benjamin, 1975.
[2] D. Montanari *et al.*, *Phys. Lett. B* **697**, 288 (2011).
[3] D. Montanari *et al.*, *Phys. Rev. C* **85**, 044301 (2012).
[4] G. Bocchi *et al.*, *Phys. Rev. C* **89**, 054302 (2014).
[5] H. Abele *et al.*, *Nucl. Instrum. Methods Phys. Res. A* **562**, 407 (2006).
[6] G. Bocchi *et al.*, *Phys. Lett. B* **760**, 273 (2016).
[7] W. Urban *et al.*, *Phys. Rev. C* **62**, 027301 (2000); **79**, 037304 (2009).
[8] J.-M. Régis *et al.*, *Nucl. Instrum. Methods Phys. Res. A* **763**, 210 (2014).
[9] G. Colò *et al.*, *Phys. Rev. C* **95**, 034303 (2017).
[10] B.A. Brown, *Phys. Rev. C* **58**, 220 (1998).